

Supporting Information

Unleashing the Power of Non-Toxic Zn-Guanidine Catalysts for Sustainable Lactide Polymerization through Smart Modeling

Jinbo Ke^{a, ‡}, Niclas Conen^{b, ‡}, Filip Latz^b, Jan Niclas Neumann^a, Dr. Martin Fuchs^a, Dr. Alexander Hoffmann^a, Prof. Dr. Andreas Jupke^{*b} and Prof. Dr. Sonja Herres-Pawlis^{*a}

a: Institute of Inorganic Chemistry, RWTH Aachen University, Landoltweg 1A, 52074 Aachen, Germany, E-mail: sonja.herres-pawlis@ac.rwth-aachen.de

b: Fluid Process Engineering (AVT.FVT), RWTH Aachen University, Forckenbeckstraße 51, 52074 Aachen, Germany, E-mail: andreas.jupke@avt.rwth-aachen.de

‡: These authors contributed equally to this work.

Contents

General information and methods	3
Experimental data	5
Determination of the Lactide Conversion	17
Model equations	18
Reference	28

General information and methods

If not mentioned specifically, all steps were carried out under an inert atmosphere using nitrogen or argon, which was further dried using P_4O_{10} granulate. Standard Schlenk and glovebox procedures were used with the glassware dried at 150 °C overnight prior to use.

The chemicals used were purchased from either Alfa Aesar, Arcos Organics, abcr GmbH, Carl Roth GmbH & Co. KG, Sigma Aldrich, TCI Deutschland GmbH or Thermo Fisher Scientific in analytical grades and used without further purification unless mentioned otherwise. The chemicals in fluid aggregation were degassed by the freeze-pump-thaw (FPT) method and stored in a N_2 filled glovebox prior to use. Solvents were purchased in technical grades and used without further purification. PURALACT® L polymer grade was donated by Total Corbion PLA in technical grade (water < 0.01 %, free acid = 0.54 meq kg⁻¹), which was recrystallized from toluene, dried in vacuo and stored in a N_2 filled glovebox prior to polymerization.

The main chemicals were listed as follows:

Chemicals	Manufacturer/Provider	Comments
L-lactide (LA)	Total Corbion PLA	recrystallized prior to polymerization
ZnCl ₂ (TMGasme) (C1)	self-made	from our previous project ^[S1]
1-hexanol (Col1)	Thermo Fisher Scientific	FPT prior to use
1,4-benzenedimethanol (Col2)	TCI Deutschland GmbH	/
<i>p</i> -Methyl benzyl alcohol	TCI Deutschland GmbH	recrystallized prior to use
ZnCl ₂	Alfa Aesar	/

NMR spectroscopy

NMR spectra were recorded on a Bruker Avance III (400 MHz) or a Bruker Avance II (400 MHz) nuclear resonance spectrometer at room temperature. The reference of the resonances was made against the residual signals of the deuterated solvent [$CDCl_3$: $\delta(^1H) = 7.26$ ppm]. The data for ¹H NMR spectra is reported as chemical shift δ (ppm) (multiplicity, coupling constant (Hz), integration). The couplings are expressed by s = singlet, d = doublet, t = triplet, q = quartet, m = multiplet or combinations thereof. For the Bruker Avance III HD 400 the software Topspin (Version 3.5 pl 7) from Bruker and for the Bruker Avance II 400 the software TopSpin (Version 2.1) from Bruker were used for data acquisition. For visualization and examination of the NMR spectra the software MestReNova (Version 14.2.3-29241) from Mestrelab Research was used.

Gel permeation chromatography (GPC)

The average molar masses and the dispersity of the polymers were examined *via* GPC. A GPCmax VE-2001 from Viscotek was used, applying a flow rate of 1 ml/min at 25 °C with THF as the mobile phase. The used apparatus consists of a

HPLC pump in combination with two Malvern Viscotek T columns (porous styrene divinylbenzene copolymer) with a max. pore size of 500 and 5000 Å and a refractive index detector (VE-3580). To evaluate the chromatographic results, a conventional calibration was used. To determine the molar mass of PLA a correction factor of 0.58 was used relative to polystyrene according to literature.^[S2] The software Omniseq – 5.12 was used for data acquisition.

In situ Raman spectroscopy

The polymerization experiments were monitored *via in situ* Raman spectroscopy using a Kaiser RXN 1 spectrometer. All spectra were collected under the polymerization parameters (Ar, 150 °C) at a wavelength of 785 nm and detected using a TE-Cooled 1024 CCD detector. The used stainless-steel reactor was equipped with an immersion probe with a sapphire lens (d = 0.1 mm), optimized to measure biphasic reaction systems and an overhead stirrer by Premex Reactor AG (PRE 1946 with a torsional moment of 20 Ncm⁻¹). The software iC Raman – V 4.1 was used for data acquisition. The Peaxact Software 5.0 was used to evaluate the obtained time-resolved data, integrating the characteristic peaks for lactide (656 cm⁻¹) and polylactide (872 cm⁻¹) to calculate the kinetic data.^[S3]



Figure S1: Experimental setup of the *in situ* Raman polymerization reactor.

Experimental data

Lactide ROP with C1

Table S1: General converted molar masse used for polymerization.

[LA]/[Co1]/[C1] ^a	molar mass [mmol]			
	X = 3.31	X = 6.62	X = 10	C1
500:X:1	0.367	0.735	1.110	0.111
500:X:1	0.367	0.735	1.110	0.111
750:X:1	0.245	0.490	0.740	0.074
1000:X:1	0.184	0.367	0.556	0.056
1250:X:1	0.147	0.294	0.444	0.044
1500:X:1	0.122	0.245	0.370	0.037
1500:X:1	0.122	0.245	0.370	0.037
[LA]/[Co2]/[C1] ^a	Y = 1	Y = 5	Y = 10	C1
500:Y:1	0.111	0.555	1.110	0.111
500:Y:1	0.111	0.555	1.110	0.111
1000:Y:1	0.056	0.278	0.555	0.056
1500:Y:1	0.037	0.185	0.370	0.037
2000:Y:1	0.028	0.139	0.278	0.028
2500:Y:1	0.022	0.111	0.222	0.022
2500:Y:1	0.022	0.111	0.222	0.022
[LA]/[pMeBnOH]/[ZnCl ₂] ^b	/	/	pMeBnOH	ZnCl ₂
2500:10:1	/	/	0.222	0.022

a) Conditions: solvent free polymerization in stainless steel reactor with overhead stirring (260 rpm) for 90 min at 150 °C, recrystallized L-lactide (55.5 mmol, 8.0 g). b) Conditions: recrystallized L-lactide (55.5 mmol, 8.0 g); The solid mixture was divided evenly, each portion for a solvent free polymerization in Schlenk tube contained a magnetic stirrer with stirring speed 260 rpm at 150 °C for different reaction time.

Table S2: Weighed quantity and acquired polymerization data for C1 without co-initiator.^a

	[LA]/[C1]	m(C1) [mg]	C _{NMR} [%] ^b	C _{Raman} [%] ^c	M _{n,theo.} [g mol ⁻¹] ^d	M _{n,exp.} [g mol ⁻¹] ^e	D
1 ^f	500:1	42.8	58	60	42000	25700	1.5
2 ^f	500:1	42.8	55	50	39300	19000	1.7
3	750:1	28.5	39	39	41800	20900	1.5
4	1000:1	21.4	30	29	43400	15800	1.5
5	1250:1	17.1	22	20	40100	9300	1.6
6 ^f	1500:1	14.3	18	16	38700	6400	1.7
7 ^f	1500:1	14.3	20	18	44200	7700	1.6

a) Conditions: solvent free polymerization in stainless steel reactor with overhead stirring (260 rpm) for 90 min at 150 °C, recrystallized L-lactide (8.0 g). b) Dissolved in CDCl₃ and determined *via* ¹H-NMR spectroscopy. c) Determined

via Raman spectroscopy. d) via $([LA]/[C1]) \times c_{NMR} \times M(LA)$. e) Determined via GPC (in THF) with conventional calibration and a corrector factor of 0.58 for PLA.^[S2] f) Data used for error analysis of the parametrization.

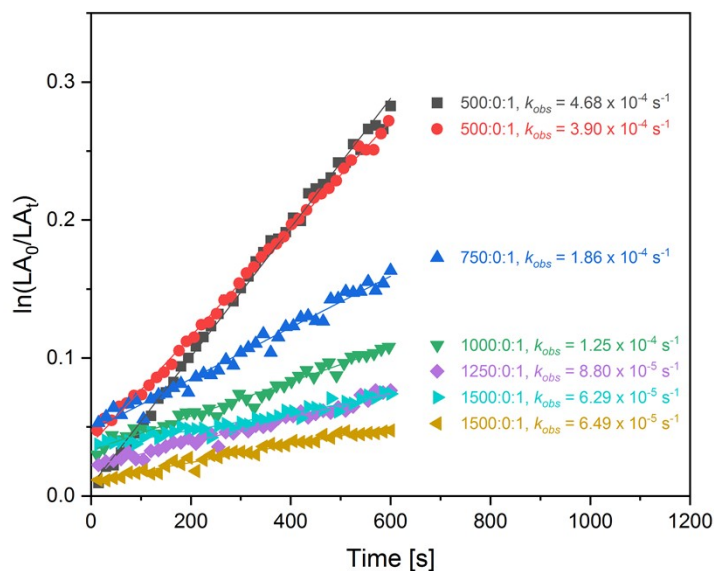


Figure S2: Initial ranges of the semilogarithmic plot of conversion versus time of ROP of L-lactide with **C1** without co-initiator to determine the apparent rate constant k_{obs} .

Based on the above Figure S2, each apparent rate constant k_{obs} from the initial ranges is plotted over the catalyst concentration to determine the reaction rate constant k_p (Figure S3). To reduce the fitting error, the experiments at the [LA]/[cat.]-ratio 500:1 as well as 1500:1 were performed twice. The larger k_{obs} between the two k_{obs} from 500:1 was grouped together with the smaller one between the two k_{obs} from 1500:1 ($k_{p,1}$, red dots), the remaining pairs were kept together ($k_{p,2}$, blue dots). And then the averaged k_{obs} was used for the determination of k_p (black dots), which contains the error bar from the repeated experiments.

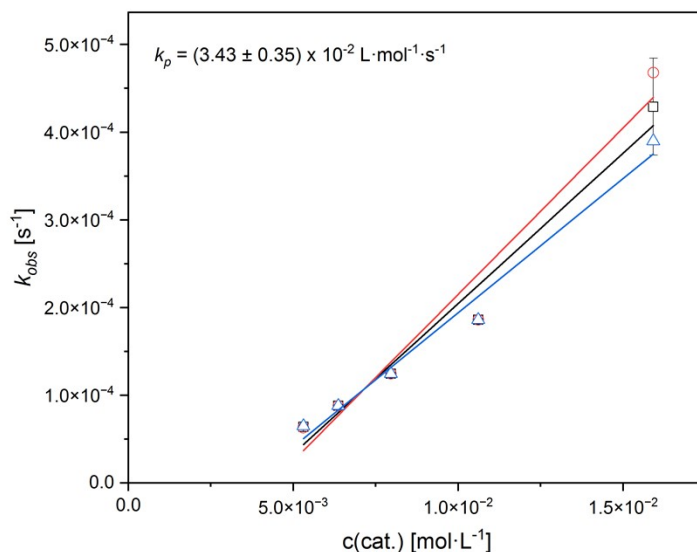


Figure S3: Determination of the reaction rate constant k_p of ROP of L-lactide with **C1** without co-initiator by plotting the apparent rate coefficient k_{obs} from the initial ranges over the catalyst concentration. a) black dots for determination of k_p . b) red dots for $k_{p,1}$. c) blue dots for $k_{p,2}$.

Table S3: Weighed quantity and acquired polymerization data for **C1** and 3.31 eq 1-hexanol (**Col1**).^a

	[LA]/[Col1]/[C1]	$m(\mathbf{C1})$ [mg]	$V(1\text{-hexanol})$ [μL]	C_{NMR} [%] ^b	C_{Raman} [%] ^c	$M_{n,\text{theo.}}$ [g mol^{-1}] ^d	$M_{n,\text{exp.}}$ [g mol^{-1}] ^e	\bar{D}
1^f	500:3.31:1	42.8	46.1	82	78	13700	19700	1.1
2^f	500:3.31:1	42.8	46.1	79	80	13200	23200	1.3
3	750:3.31:1	28.5	30.7	61	60	15300	24000	1.4
4	1000:3.31:1	21.4	23.1	50	59	16700	14200	1.1
5	1250:3.31:1	17.1	18.4	35	35	14500	15400	1.1
6^f	1500:3.31:1	14.3	15.4	20	20	10200	6200	1.7
7^f	1500:3.31:1	14.3	15.4	27	27	13500	7400	1.6

a) Conditions: solvent free polymerization in stainless steel reactor with overhead stirring (260 rpm) for 90 min at 150 °C, recrystallized L-lactide (8.0 g). b) Dissolved in CDCl_3 and determined *via* $^1\text{H-NMR}$ spectroscopy. c) Determined *via* Raman spectroscopy. d) *via* $([\text{LA}]/[\mathbf{C1}]) \times C_{\text{NMR}} \times M(\text{LA})$. e) Determined *via* GPC (in THF) with conventional calibration and a corrector factor of 0.58 for PLA.^[S2] f) Data used for error analysis of the parametrization.

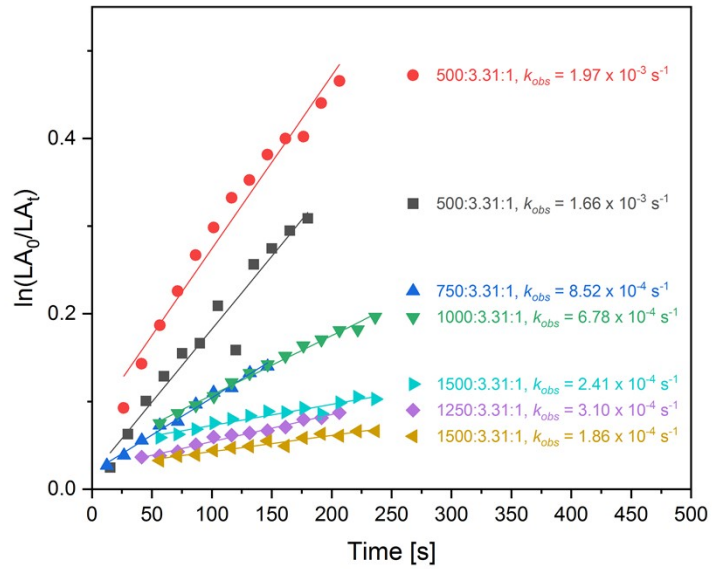


Figure S4: Initial ranges of the semilogarithmic plot of conversion versus time of ROP of L-lactide with **C1** and 3.31 eq 1-hexanol (**Col1**) to determine the apparent rate constant k_{obs} .

According to the analysis method mentioned above:

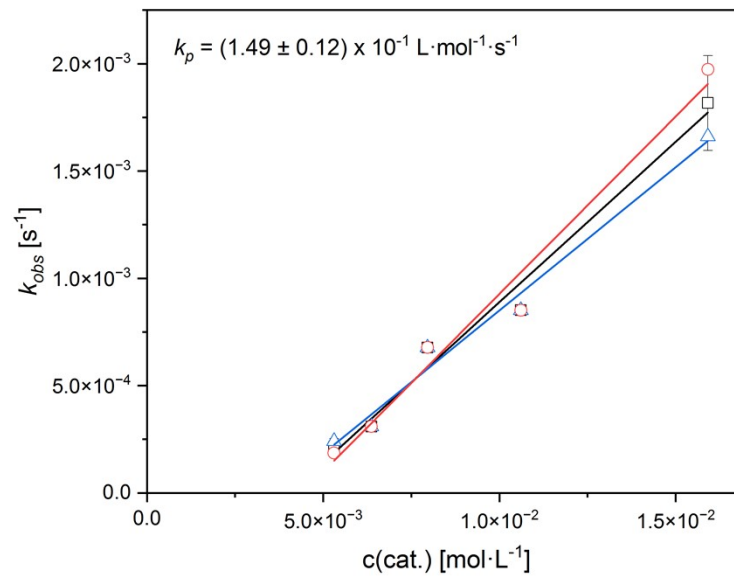


Figure S5: Determination of the reaction rate constant k_p of ROP of L-lactide with **C1** and 3.31 eq 1-hexanol (**Col1**) by plotting the apparent rate coefficient k_{obs} from the initial ranges over the catalyst concentration. a) black dots for determination of k_p . b) red dots for $k_{p,1}$. c) blue dots for $k_{p,2}$.

Table S4: Weighed quantity and acquired polymerization data for **C1** and 6.62 eq 1-hexanol (**Col1**).^a

	[LA]/[Col1]/[C1]	$m(\mathbf{C1})$ [mg]	$V(1\text{-hexanol})$ [μL]	C_{NMR} [%] ^b	C_{Raman} [%] ^c	$M_{n,\text{theo.}}$ [g mol^{-1}] ^d	$M_{n,\text{exp.}}$ [g mol^{-1}] ^e	\bar{D}
1^f	500:6.62:1	42.8	92.2	89	88	8500	10500	1.1
2^f	500:6.62:1	42.8	92.2	90	83	8500	10800	1.1
3	750:6.62:1	28.5	61.5	84	86	11900	18500	1.1
4	1000:6.62:1	21.4	46.1	76	69	14300	21200	1.1
5	1250:6.62:1	17.1	36.9	63	57	14800	18500	1.1
6^f	1500:6.62:1	14.3	30.7	45	41	12700	17700	1.1
7^f	1500:6.62:1	14.3	30.7	41	41	11700	16500	1.1

a) Conditions: solvent free polymerization in stainless steel reactor with overhead stirring (260 rpm) for 90 min at 150 °C, recrystallized L-lactide (8.0 g). b) Dissolved in CDCl_3 and determined *via* $^1\text{H-NMR}$ spectroscopy. c) Determined *via* Raman spectroscopy. d) *via* $([\text{LA}]/[\mathbf{C1}]) \times C_{\text{NMR}} \times M(\text{LA})$. e) Determined *via* GPC (in THF) with conventional calibration and a corrector factor of 0.58 for PLA.^[S2] f) Data used for error analysis of the parametrization.

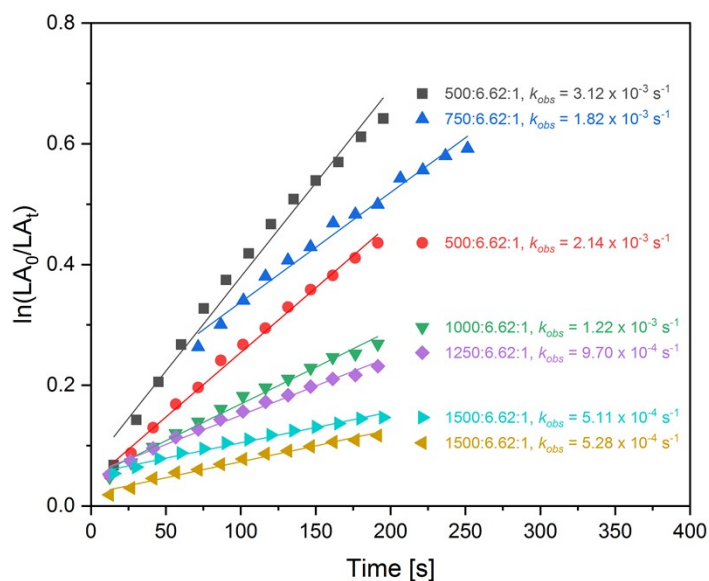


Figure S6: Initial ranges of the semilogarithmic plot of conversion versus time of ROP of L-lactide with **C1** and 6.62 eq 1-hexanol (**Col1**) to determine the apparent rate constant k_{obs} .

According to the analysis method mentioned above:

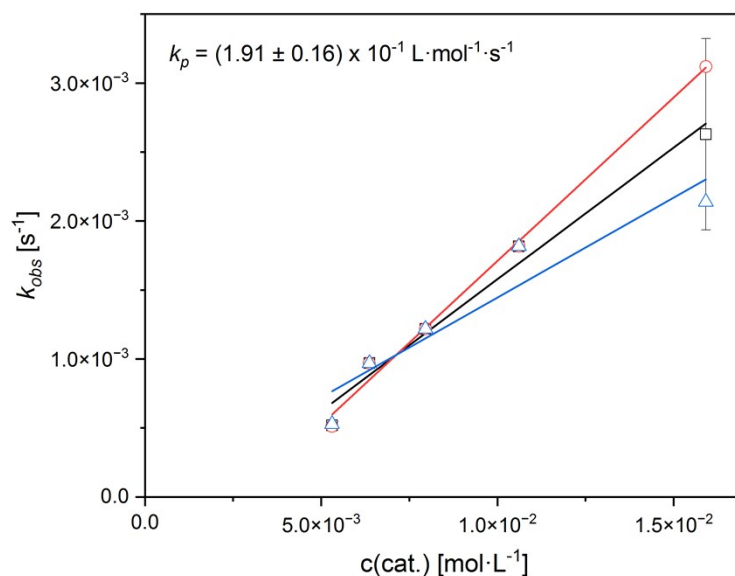


Figure S7: Determination of the reaction rate constant k_p of ROP of L-lactide with **C1** and 6.62 eq 1-hexanol (**Col1**) by plotting the apparent rate coefficient k_{obs} from the initial ranges over the catalyst concentration. a) black dots for determination of k_p . b) red dots for $k_{p,1}$. c) blue dots for $k_{p,2}$.

Table S5: Weighed quantity and acquired polymerization data for **C1** and 10 eq 1-hexanol (**Col1**).^a

	[LA]/[Col1]/[C1]	$m(\mathbf{C1})$ [mg]	$V(1\text{-hexanol})$ [μL]	C_{NMR} [%] ^b	C_{Raman} [%] ^c	$M_{n,\text{theo.}}$ [g mol^{-1}] ^d	$M_{n,\text{exp.}}$ [g mol^{-1}] ^e	\mathcal{D}
1^f	500:10:1	42.8	139.4	93	91	6100	7800	1.1
2^f	500:10:1	42.8	139.4	90	89	5900	11600	1.2
3	750:10:1	28.5	92.9	79	82	7800	10500	1.1
4	1000:10:1	21.4	69.7	81	79	10600	12800	1.1
5	1250:10:1	17.1	55.7	73	73	11900	13600	1.1
6^f	1500:10:1	14.3	46.5	54	52	10700	17800	1.1
7^f	1500:10:1	14.3	46.5	49	45	9600	10400	1.1

a) Conditions: solvent free polymerization in stainless steel reactor with overhead stirring (260 rpm) for 90 min at 150 °C, recrystallized L-lactide (8.0 g). b) Dissolved in CDCl_3 and determined *via* $^1\text{H-NMR}$ spectroscopy. c) Determined *via* Raman spectroscopy. d) *via* $([\text{LA}]/[\mathbf{C1}]) \times c_{\text{NMR}} \times M(\text{LA})$. e) Determined *via* GPC (in THF) with conventional calibration and a corrector factor of 0.58 for PLA.^[S2] f) Data used for error analysis of the parametrization.

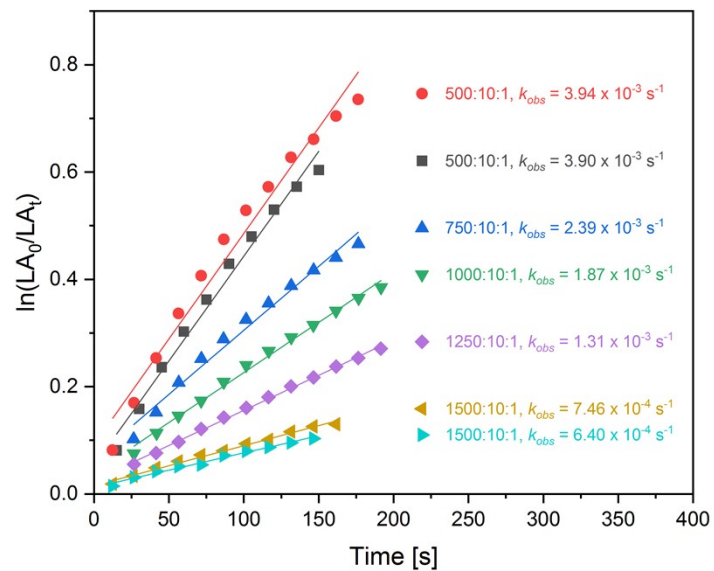


Figure S8: Initial ranges of the semilogarithmic plot of conversion versus time of ROP of L-lactide with **C1** and 10 eq 1-hexanol (**Co11**) to determine the apparent rate constant k_{obs} .

According to the analysis method mentioned above:

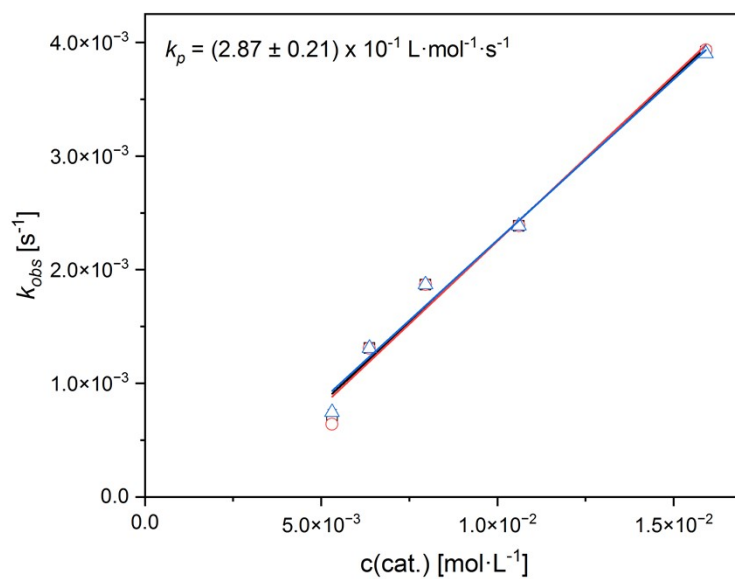


Figure S9: Determination of the reaction rate constant k_p of ROP of L-lactide with **C1** and 10 eq 1-hexanol (**Co11**) by plotting the apparent rate coefficient k_{obs} from the initial ranges over the catalyst concentration. a) black dots for determination of k_p . b) red dots for $k_{p,1}$. c) blue dots for $k_{p,2}$.

Table S6: Weighed quantity and acquired polymerization data for **C1** and 1 eq 1,4-benzenedimethanol (**Co12**).^a

	[LA]/[Co12]/[C1]	$m(\text{C1})$ [mg]	$m(\text{diol})$ [mg]	C_{NMR} [%] ^b	C_{Raman} [%] ^c	$M_{n,\text{theo.}}$ [g mol ⁻¹] ^d	$M_{n,\text{exp.}}$ [g mol ⁻¹] ^e	\bar{D}
1^f	500:1:1	42.8	15.3	82	82	29400	40600	1.4
2^f	500:1:1	42.8	15.3	73	71	26300	33400	1.5
3	1000:1:1	21.4	7.7	46	43	32800	23600	1.6
4	1500:1:1	14.3	5.1	41	38	44200	24600	1.6
5	2000:1:1	10.7	3.8	25	25	35900	17500	1.6
6^f	2500:1:1	8.6	3.1	19	16	35100	9500	2.0
7^f	2500:1:1	8.6	3.1	21	18	37900	11700	1.9

a) Conditions: solvent free polymerization in stainless steel reactor with overhead stirring (260 rpm) for 90 min at 150 °C, recrystallized L-lactide (8.0 g). b) Dissolved in CDCl₃ and determined *via* ¹H-NMR spectroscopy. c) Determined *via* Raman spectroscopy. d) *via* ([LA]/[C1]) × C_{NMR} × $M(\text{LA})$. e) Determined *via* GPC (in THF) with conventional calibration and a corrector factor of 0.58 for PLA.^[S2] f) Data used for error analysis of the parametrization.

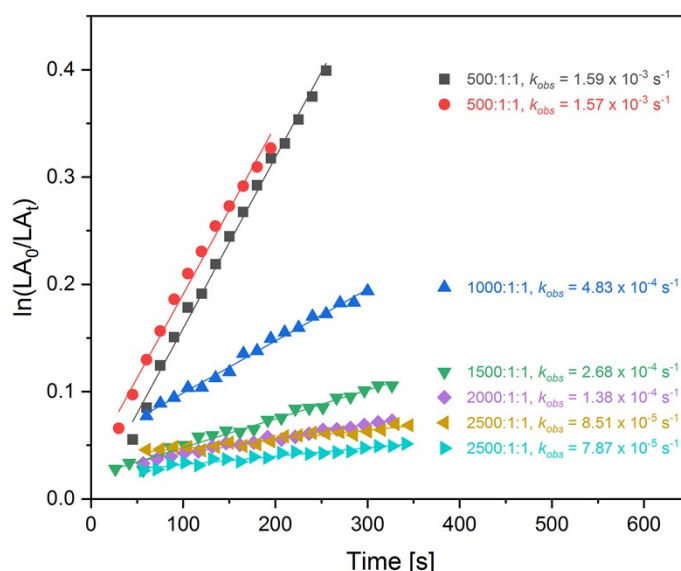


Figure S10: Initial ranges of the semilogarithmic plot of conversion versus time of ROP of L-lactide with **C1** and 1 eq 1,4-benzenedimethanol (**Co12**) to determine the apparent rate constant k_{obs} .

Similar to the analysis method mentioned above for **Co11**, each apparent rate coefficient k_{obs} from the initial ranges is plotted over the catalyst concentration to determine the reaction rate constant k_p (Figure S11). But the repeated experiments were at the [LA]/[cat.]-ratio 500:1 as well as 2500:1. Thus, the k_{obs} grouped together are from 500:1 and 2500:1. Other than that, the rest of the processes were the same.

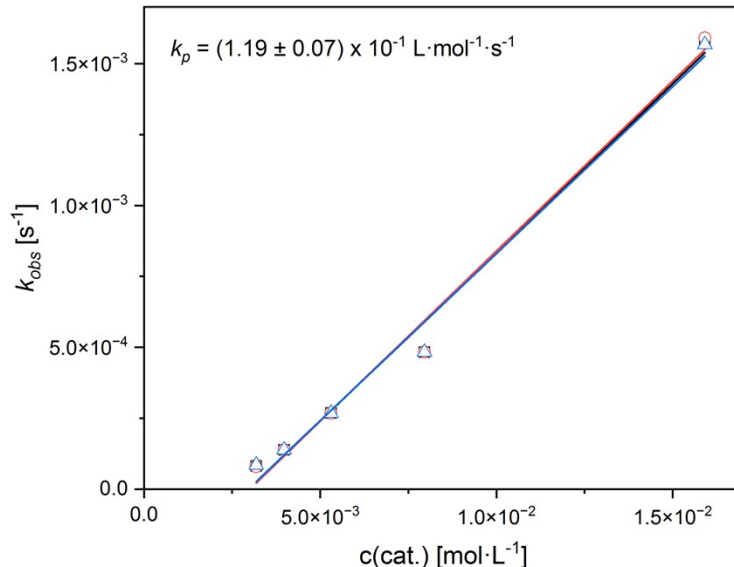


Figure S11: Determination of the reaction rate constant k_p of ROP of L-lactide with **C1** and 1 eq 1,4-benzenedimethanol (**CoI2**) by plotting the apparent rate coefficient k_{obs} from the initial ranges over the catalyst concentration. a) black dots for determination of k_p . b) red dots for $k_{p,1}$. c) blue dots for $k_{p,2}$.

Table S7: Weighed quantity and acquired polymerization data for **C1** and 5 eq 1,4-benzenedimethanol (**CoI2**).^a

	[LA]/[CoI2]/[C1]	$m(\mathbf{C1})$ [mg]	$m(\text{diol})$ [mg]	C_{NMR} [%] ^b	C_{Raman} [%] ^c	$M_{n,\text{theo.}}$ [g mol ⁻¹] ^d	$M_{n,\text{exp.}}$ [g mol ⁻¹] ^e	\bar{D}
1^f	500:5:1	42.8	76.7	93	94	11200	15900	1.1
2^f	500:5:1	42.8	76.7	95	95	11400	16200	1.1
3	1000:5:1	21.4	38.3	80	78	19100	24400	1.1
4	1500:5:1	14.3	25.6	60	58	21700	23300	1.2
5	2000:5:1	10.7	19.2	46	43	22200	20500	1.2
6^f	2500:5:1	8.6	15.3	25	21	15100	7900	1.5
7^f	2500:5:1	8.6	15.3	34	34	20500	19200	1.4

a) Conditions: solvent free polymerization in stainless steel reactor with overhead stirring (260 rpm) for 90 min at 150 °C, recrystallized L-lactide (8.0 g). b) Dissolved in CDCl₃ and determined *via* ¹H-NMR spectroscopy. c) Determined *via* Raman spectroscopy. d) *via* ([LA]/[C1]) × C_{NMR} × $M(\text{LA})$. e) Determined *via* GPC (in THF) with conventional calibration and a corrector factor of 0.58 for PLA.^[S2] f) Data used for error analysis of the parametrization.

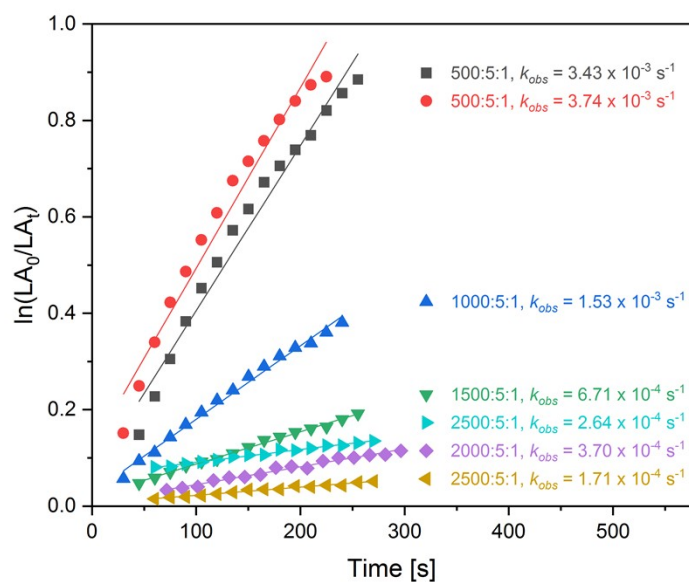


Figure S12: Initial ranges of the semilogarithmic plot of conversion versus time of ROP of L-lactide with **C1** and 5 eq 1,4-benzenedimethanol (**Co12**) to determine the apparent rate constant k_{obs} .

According to the analysis method mentioned above:

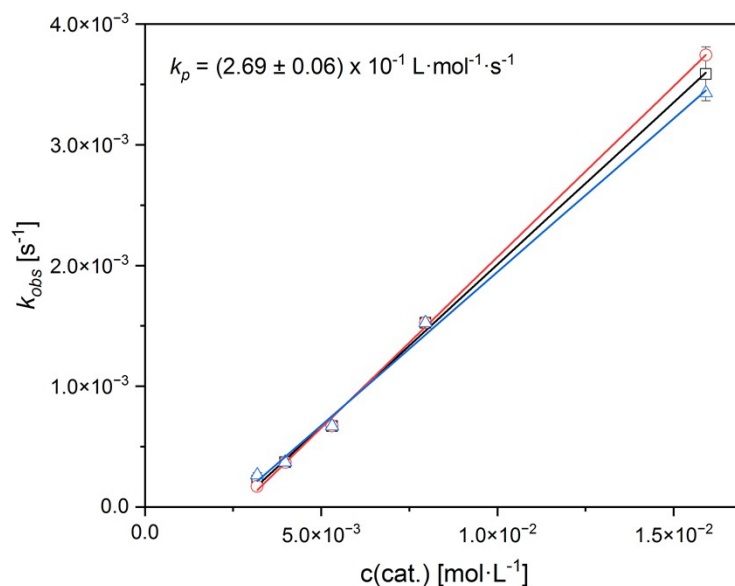


Figure S13: Determination of the reaction rate constant k_p of ROP of L-lactide with **C1** and 5 eq 1,4-benzenedimethanol (**Co12**) by plotting the apparent rate coefficient k_{obs} from the initial ranges over the catalyst concentration. a) black dots for determination of k_p . b) red dots for $k_{p,1}$. c) blue dots for $k_{p,2}$.

Table S8: Weighed quantity and acquired polymerization data for **C1** and 10 eq 1,4-benzenedimethanol (**CoI2**).^a

	[LA]/[CoI2]/[C1]	<i>m</i> (C1) [mg]	<i>m</i> (diol) [mg]	<i>C</i> _{NMR} [%] ^b	<i>C</i> _{Raman} [%] ^c	<i>M</i> _{n,theo.} [g mol ⁻¹] ^d	<i>M</i> _{n,exp.} [g mol ⁻¹] ^e	<i>D</i>
1^f	500:10:1	42.8	153.4	96	93	6300	7700	1.1
2^f	500:10:1	42.8	153.4	95	93	6200	11300	1.1
3	1000:10:1	21.4	76.7	80	78	10400	16500	1.0
4	1500:10:1	14.3	51.1	70	68	13700	25600	1.1
5	2000:10:1	10.7	38.3	52	50	13600	19800	1.1
6^f	2500:10:1	8.6	30.7	40	41	13200	19200	1.1
7^f	2500:10:1	8.6	30.7	53	54	17300	19600	1.1

a) Conditions: solvent free polymerization in stainless steel reactor with overhead stirring (260 rpm) for 90 min at 150 °C, recrystallized L-lactide (8.0 g). b) Dissolved in CDCl₃ and determined *via* ¹H-NMR spectroscopy. c) Determined *via* Raman spectroscopy. d) *via* ([LA]/[C1]) × *C*_{NMR} × *M*(LA). e) Determined *via* GPC (in THF) with conventional calibration and a corrector factor of 0.58 for PLA.^[S2] f) Data used for error analysis of the parametrization.

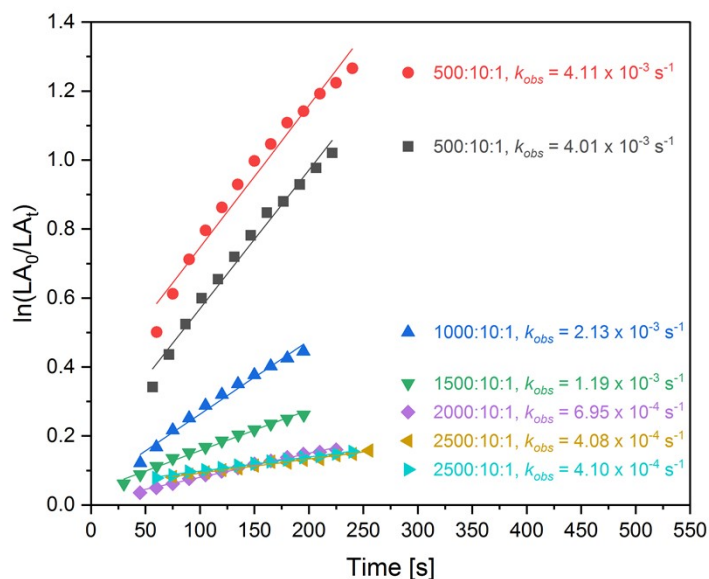


Figure S14: Initial ranges of the semilogarithmic plot of conversion versus time of ROP of L-lactide with **C1** and 10 eq 1,4-benzenedimethanol (**CoI2**) to determine the apparent rate constant *k*_{obs}.

According to the analysis method mentioned above:

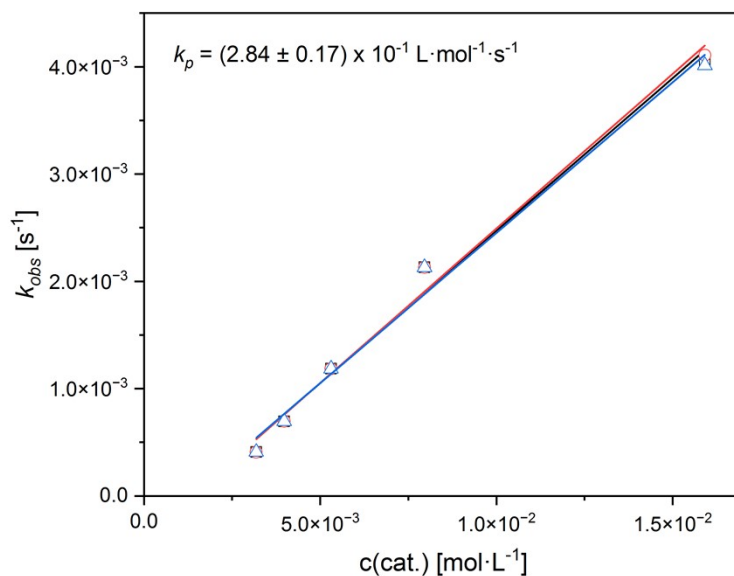


Figure S15: Determination of the reaction rate constant k_p of ROP of L-lactide with **C1** and 10 eq 1,4-benzenedimethanol (**Co12**) by plotting the apparent rate coefficient k_{obs} from the initial ranges over the catalyst concentration. a) black dots for determination of k_p . b) red dots for $k_{p,1}$. c) blue dots for $k_{p,2}$.

The conversion of L-lactide from the reaction in Schlenk tubes was determined by $^1\text{H-NMR}$ spectrum, and hence the corresponding apparent rate constant k_{obs} was determined:

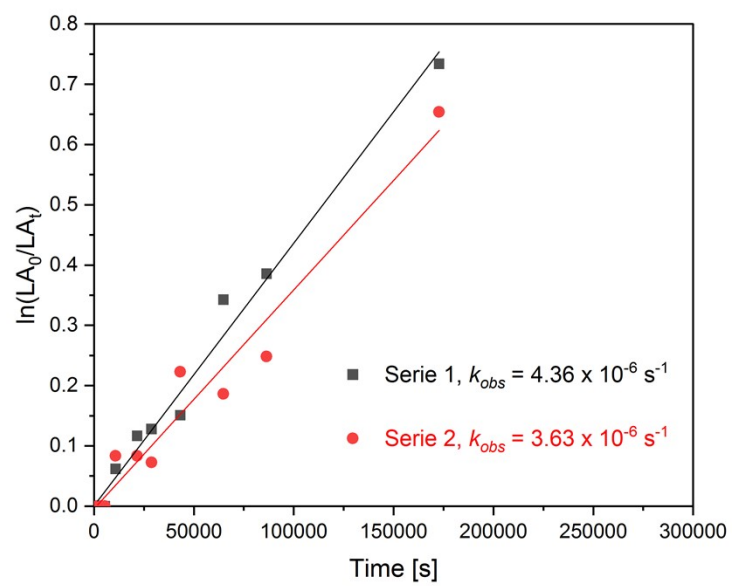


Figure S16: Semilogarithmic plot of conversion versus time of ROP of L-lactide with $ZnCl_2$ and 10 eq *p*-methylbenzylalcohol to determine the apparent rate constant k_{obs} .

Determination of the Lactide Conversion

NMR Spectroscopy

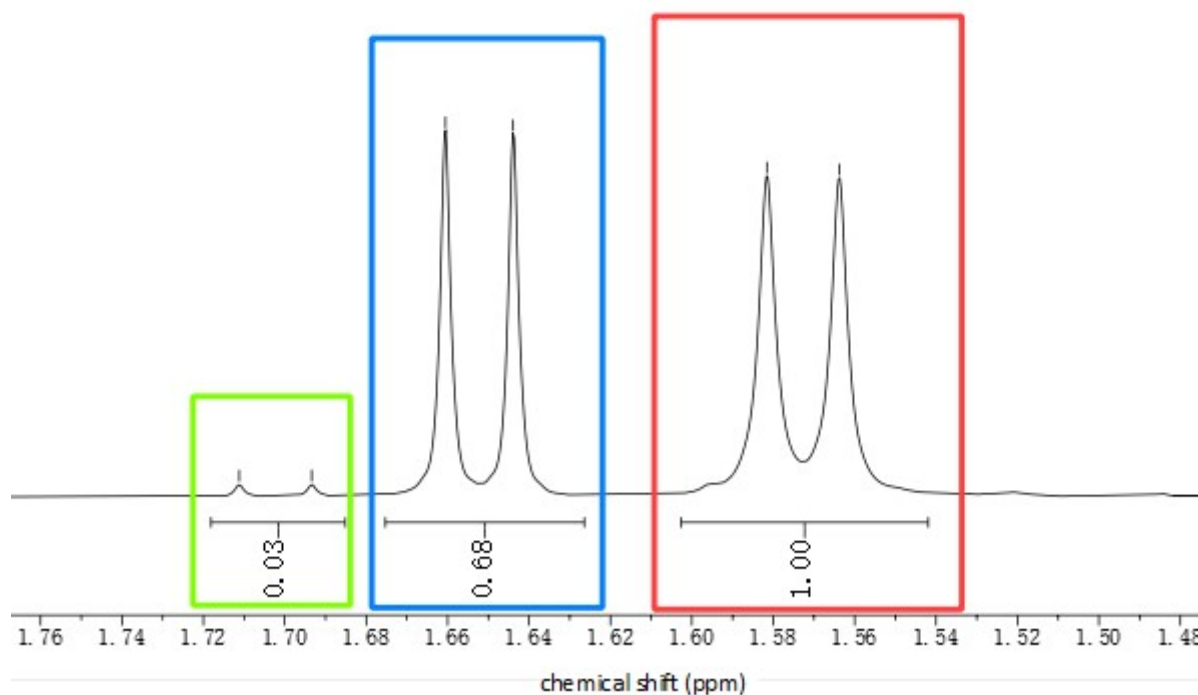


Figure S17: Exemplary ^1H -NMR spectrum for a [LA]/[CoI2]/[C1]-ratio of 1500:5:1 after 90 min with the relevant signals of the CH_3 -groups in PLA (red), L-lactide (blue) and meso-lactide (green) used to calculate the L-lactide conversion (c_{NMR}) according to equation **eq S1** below.

Using ^1H -NMR spectroscopy the L-lactide conversion (c_{NMR}) was calculated according to equation **eq S1**:

$$c_{\text{NMR}} = \frac{\int_{\text{PLA}}}{(\int_{\text{PLA}} + \int_{\text{LLA}} + \int_{\text{mesoLA}})} \times 100 \quad (\text{eq S1})$$

Model equations

Mono-functional co-initiator

Mass balance equations for small molecules (isochoric reaction, no in- and outgoing flows)

$$\frac{dM}{dt} = -k_{C,p}M\mu_0^{R_C} + k_{C,d}(\mu_0^{R_C} - R_{C,1} - R_{C,0}) - k_{CR,p}M\mu_0^{R_{CR}} + k_{CR,d}(\mu_0^{R_{CR}} - R_{CR,1} - R_{CR,0}) - k_{MC}CM \quad (1)$$

$$\frac{dC}{dt} = -k_{C,al}C\mu_0^D + k_{C,a2}AC\mu_0^{R_C} - k_{MC}CM \quad (2)$$

$$\frac{dA_C}{dt} = k_{C,al}C\mu_0^D - k_{C,a2}AC\mu_0^{R_C} \quad (3)$$

$$\frac{dCR}{dt} = -k_{CR,al}CR\mu_0^D + k_{CR,a2}ACR\mu_0^{R_{CR}} + k_{MC}CM \quad (4)$$

$$\frac{dA_{CR}}{dt} = k_{CR,al}CR\mu_0^D - k_{CR,a2}ACR\mu_0^{R_{CR}} \quad (5)$$

Population balance equations:

$$\begin{aligned}
\frac{dR_{C,n}}{dt} = & k_{C,a1}CD_n - k_{C,a2}A_C R_{C,n} + (1 - \delta_{n,0})(1 - \delta_{n,1})(k_{C,p}R_{C,n-2}M - k_{C,d}R_{C,n}) + k_{C,d}R_{C,n+2} \\
& - k_{C,p}R_{C,n} - k_s R_{C,n} (\mu_0^D + \mu_0^{RCR}) + k_s (D_n + R_{C,n}) \mu_0^{RC} \\
& - k_{te} \{ R_{C,n} (\mu_1^{RC} - \mu_0^{RC} + R_{C,0}) - (1 - \delta_{n,0}) \mu_0^{RC} \sum_{j=n+1}^{\infty} R_{C,j} + (1 - \delta_{n,0})(1 - \delta_{n,1})(n-1)R_{C,n} \mu_0^{RC} \\
& - (1 - \delta_{n,0})^{n-1} \sum_{i=0}^{\infty} R_{C,i} \sum_{k=n+1-i}^{\infty} R_{C,k} + R_{C,n} (\mu_1^{RCR} - \mu_0^{RCR} + R_{CR,0}) - (1 - \delta_{n,0}) \mu_0^{RC} \sum_{i=n+1}^{\infty} R_{CR,i} \\
& + R_{C,n} (\mu_1^D - \mu_0^D + D_0) - (1 - \delta_{n,0}) \mu_0^{RC} \sum_{i=n+1}^{\infty} D_i + R_{C,n} (\mu_1^G - \mu_0^G + G_0) - (1 - \delta_{n,0}) \mu_0^{RC} \sum_{i=n+1}^{\infty} G_i \} \\
& - k_{de}(n-1)R_{C,n} + k_{de} \sum_{i=n+1}^{\infty} R_{C,i} \tag{6}
\end{aligned}$$

$$\begin{aligned}
\frac{dR_{CR,n}}{dt} = & k_{CR,a1}CRD_n - k_{CR,a2}A_{CR}R_{CR,n} + (1 - \delta_{n,0})(1 - \delta_{n,1})(k_{CR,p}R_{CR,n-2}M - k_{CR,d}R_{CR,n}) + k_{CR,d}R_{CR,n+2} \\
& - k_{CR,p}R_{CR,n} - k_s R_{CR,n} (\mu_0^D + \mu_0^{RC}) + k_s (D_n + R_{C,n}) \mu_0^{RCR} \\
& - k_{te} \{ R_{CR,n} (\mu_1^{RCR} - \mu_0^{RCR} + R_{CR,0}) - (1 - \delta_{n,0}) \mu_0^{RCR} \sum_{j=n+1}^{\infty} R_{CR,j} + (1 - \delta_{n,0})(1 - \delta_{n,1})(n-1)R_{CR,n} \mu_0^{RCR} \\
& - (1 - \delta_{n,0})^{n-1} \sum_{i=0}^{\infty} R_{CR,i} \sum_{k=n+1-i}^{\infty} R_{CR,k} + R_{CR,n} (\mu_1^{RC} - \mu_0^{RC} + R_{C,0}) - (1 - \delta_{n,0}) \mu_0^{RCR} \sum_{i=n+1}^{\infty} R_{C,i} \\
& + R_{CR,n} (\mu_1^D - \mu_0^D + D_0) - (1 - \delta_{n,0}) \mu_0^{RCR} \sum_{i=n+1}^{\infty} D_i + R_{CR,n} (\mu_1^G - \mu_0^G + G_0) - (1 - \delta_{n,0}) \mu_0^{RCR} \sum_{i=n+1}^{\infty} G_i \} \\
& - k_{de}(n-1)R_{CR,n} + k_{de} \sum_{i=n+1}^{\infty} R_{CR,i} \tag{7}
\end{aligned}$$

$$\begin{aligned}
\frac{dD_n}{dt} = & -k_{C,a1}CD_n + k_{C,a2}A_C R_{C,n} - k_{CR,a1}CRD_n + k_{CR,a2}A_{CR}R_{CR,n} + k_{CM}\delta_{n,2}CM + k_s (R_{C,n} + R_{CR,n}) \mu_0^D \\
& - k_s D_n (\mu_0^{RC} + \mu_0^{RCR}) + k_{te} (1 - \delta_{n,0}) \sum_{i=0}^{n-1} (R_{C,i} + R_{CR,i}) \sum_{k=n+1-i}^{\infty} D_k \\
& - k_{te} (1 - \delta_{n,0})(1 - \delta_{n,1})(n-1)D_n (\mu_0^{RC} + \mu_0^{RCR}) - k_{de}(n-1)D_n + k_{de} \sum_{i=n+1}^{\infty} D_i \tag{8}
\end{aligned}$$

$$\begin{aligned}
\frac{dG_n}{dt} = & k_{te} (1 - \delta_{n,0}) (\mu_0^{RC} + \mu_0^{RCR}) \sum_{i=n+1}^{\infty} G_i - k_{te} (1 - \delta_{n,0})(1 - \delta_{n,1})(n-1)G_n (\mu_0^{RC} + \mu_0^{RCR}) \\
& - 2k_{de} (1 - \delta_{n,0})(1 - \delta_{n,1})(n-1)G_n + 2k_{de} (1 - \delta_{n,0}) \sum_{m=n+1}^{\infty} G_m \\
& + k_{de} (1 - \delta_{n,0}) \sum_{k=n+1}^{\infty} (R_{C,k} + R_{CR,k}) + k_{de} (1 - \delta_{n,0}) \sum_{k=n+1}^{\infty} D_k \tag{9}
\end{aligned}$$

These lead to the following moment equations for moments 0 to 2:

Active chains with catalyst chain end:

$$\frac{d\mu_0^{RC}}{dt} = k_{C,a1}C\mu_0^D - k_{C,a2}A_C\mu_0^{RC} \quad (10)$$

$$\begin{aligned} \frac{d\mu_1^{RC}}{dt} = & k_{C,a1}C\mu_1^D - k_{C,a2}A_C\mu_1^{RC} + 2k_{C,p}M\mu_0^{RC} - 2k_{C,d}\mu_0^{RC} \\ & + k_s \left[-\mu_1^{RC} (\mu_0^D + \mu_0^{RCR}) + \mu_0^{RC} (\mu_1^D + \mu_1^{RCR}) \right] \\ & + k_{te} \left[-\mu_1^{RC} (\mu_1^D - \mu_0^D + \mu_1^{RCR} - \mu_0^{RCR}) + \frac{1}{2}\mu_0^{RC} (\mu_2^D - \mu_1^D + \mu_2^{RCR} - \mu_1^{RCR}) \right. \\ & \quad \left. - \mu_1^{RC} (\mu_1^G - \mu_0^G) + \frac{1}{2}\mu_0^{RC} (\mu_2^G - \mu_1^G) \right] \\ & - \frac{1}{2}k_{de} (\mu_2^{RC} - \mu_1^{RC}) \end{aligned} \quad (11)$$

$$\begin{aligned} \frac{d\mu_2^{RC}}{dt} = & k_{C,a1}C\mu_2^D - k_{C,a2}A_C\mu_2^{RC} + 4k_pM (\mu_1^{RC} + \mu_0^{RC}) + 4k_d (\mu_0^{RC} - \mu_1^{RC}) \\ & + k_s \left[-\mu_2^{RC} (\mu_0^D + \mu_0^{RCR}) + \mu_0^{RC} (\mu_2^D + \mu_2^{RCR}) \right] \\ & + k_{te} \left[\frac{1}{3}\mu_0^{RC} (\mu_1^{RC} - \mu_3^{RC}) + \mu_1^{RC} (\mu_2^{RC} - \mu_1^{RC}) - \mu_2^{RC} (\mu_1^D - \mu_0^D + \mu_1^{RCR} - \mu_0^{RCR}) \right. \\ & \quad + \frac{1}{6}\mu_0^{RC} (2\mu_3^D - 3\mu_2^D + \mu_1^D + 2\mu_3^{RCR} - 3\mu_2^{RCR} + \mu_1^{RCR}) - \mu_2^{RC} (\mu_1^G - \mu_0^G) \\ & \quad \left. + \frac{1}{6}\mu_0^{RC} (2\mu_3^G - 3\mu_2^G + \mu_1^G) \right] \\ & - \frac{1}{6}k_{de} (4\mu_3^{RC} - 3\mu_2^{RC} - \mu_1^{RC}) \end{aligned} \quad (12)$$

Active chains with catalyst residue chain end:

$$\frac{d\mu_0^{RCR}}{dt} = k_{CR,a1}CR\mu_0^D - k_{CR,a2}ACR\mu_0^{RCR} \quad (13)$$

$$\begin{aligned} \frac{d\mu_1^{RCR}}{dt} &= k_{CR,a1}CR\mu_1^D - k_{CR,a2}ACR\mu_1^{RCR} + 2k_{CR,p}M\mu_0^{RCR} - 2k_{CR,d}\mu_0^{RCR} \\ &+ k_s \left[\mu_1^{RCR} (\mu_0^D + \mu_0^{RC}) + \mu_0^{RCR} (\mu_1^D + \mu_1^{RC}) \right] \\ &+ k_{te} \left[-\mu_1^{RCR} (\mu_1^D - \mu_0^D + \mu_1^{RC} - \mu_0^{RC}) + \frac{1}{2}\mu_0^{RCR} (\mu_2^D - \mu_1^D + \mu_2^{RC} - \mu_1^{RC}) \right. \\ &\quad \left. - \mu_1^{RCR} (\mu_1^G - \mu_0^G) + \mu_0^{RCR} (\mu_2^G - \mu_1^G) \right] \\ &- \frac{1}{2}k_{de} (\mu_2^{RCR} - \mu_1^{RCR}) \end{aligned} \quad (14)$$

$$\begin{aligned} \frac{d\mu_2^{RCR}}{dt} &= k_{C,a1}CR\mu_2^D - k_{CR,a2}ACR\mu_2^{RCR} + 4k_pM (\mu_1^{RCR} + \mu_0^{RCR}) + 4k_d (\mu_0^{RCR} - \mu_1^{RCR}) \\ &+ k_s \left[-\mu_2^{RCR} (\mu_0^D + \mu_0^{RC}) + \mu_0^{RCR} (\mu_2^D + \mu_2^{RC}) \right] \\ &+ k_{te} \left[\frac{1}{3}\mu_0^{RCR} (\mu_1^{RC} - \mu_3^{RCR}) + \mu_1^{RCR} (\mu_2^{RCR} - \mu_1^{RCR}) - \mu_2^{RCR} (\mu_1^D - \mu_0^D + \mu_1^{RC} - \mu_0^{RC}) \right. \\ &\quad \left. + \frac{1}{6}\mu_0^{RCR} (2\mu_3^D - 3\mu_2^D + \mu_1^D + 2\mu_3^{RC} - 3\mu_2^{RC} + \mu_1^{RC}) - \mu_2^{RCR} (\mu_1^G - \mu_0^G) \right. \\ &\quad \left. + \frac{1}{6}\mu_0^{RCR} (2\mu_3^G - 3\mu_2^G + \mu_1^G) \right] \\ &- \frac{1}{6}k_{de} (4\mu_3^{RCR} - 3\mu_2^{RCR} - \mu_1^{RCR}) \end{aligned} \quad (15)$$

Inactive chains:

$$\frac{d\mu_0^D}{dt} = -k_{C,a1}C\mu_0^D + k_{C,a2}AC\mu_0^{RC} - k_{CR,a1}CR\mu_0^D + k_{CR,a2}ACR\mu_0^{RCR} + k_{CM}CM \quad (16)$$

$$\begin{aligned} \frac{d\mu_1^D}{dt} &= -k_{C,a1}C\mu_1^D + k_{C,a2}AC\mu_1^{RC} - k_{CR,a1}CR\mu_1^D + k_{CR,a2}ACR\mu_1^{RCR} + 2k_{CM}CM \\ &+ k_s \left[(\mu_1^{RC} + \mu_1^{RCR}) \mu_0^D - (\mu_0^{RC} + \mu_0^{RCR}) \mu_1^D \right] \\ &+ k_{te} \left[-(\mu_1^{RC} + \mu_1^{RCR}) (\mu_1^D - \mu_0^D) - \frac{1}{2} (\mu_0^{RC} + \mu_0^{RCR}) (\mu_2^D - \mu_1^D) \right] \\ &- \frac{1}{2}k_{de} (\mu_2^D - \mu_1^D) \end{aligned} \quad (17)$$

$$\begin{aligned} \frac{d\mu_2^D}{dt} &= -k_{C,a1}C\mu_2^D + k_{C,a2}AC\mu_2^{RC} - k_{CR,a1}CR\mu_2^D + k_{CR,a2}ACR\mu_2^{RCR} + 4k_{CM}CM \\ &+ k_s \left[(\mu_2^{RC} + \mu_2^{RCR}) \mu_0^D - (\mu_0^{RC} + \mu_0^{RCR}) \mu_2^D \right] \\ &+ k_{te} \left[(\mu_1^{RC} + \mu_1^{RCR}) (\mu_2^D - \mu_1^D) + (\mu_2^{RC} + \mu_2^{RCR}) (\mu_1^D - \mu_0^D) \right. \\ &\quad \left. + \frac{1}{6} (\mu_0^{RC} + \mu_0^{RCR}) (-4\mu_3^D + 3\mu_2^D + \mu_1^D) \right] \\ &- \frac{1}{6}k_{de} (4\mu_3^D - 3\mu_2^D - \mu_1^D) \end{aligned} \quad (18)$$

Terminated chains:

$$\frac{d\mu_0^G}{dt} = k_{de} \left[(\mu_1^{RC} - \mu_0^{RC}) + (\mu_1^{RCR} - \mu_0^{RCR}) + (\mu_1^D - \mu_0^D) \right] \quad (19)$$

$$\begin{aligned} \frac{d\mu_1^G}{dt} &= k_{te} \left[(\mu_1^{RC} + \mu_1^{RCR}) (\mu_1^G - \mu_0^G) - \frac{1}{2} (\mu_0^{RC} + \mu_0^{RCR}) (\mu_2^G - \mu_1^G) \right] \\ &+ k_{de} \left[(\mu_1^G - \mu_2^G) + \frac{1}{2} (\mu_2^{RC} - \mu_1^{RC}) + \frac{1}{2} (\mu_2^{RCR} - \mu_1^{RCR}) + \frac{1}{2} (\mu_2^D - \mu_1^D) \right] \end{aligned} \quad (20)$$

$$\begin{aligned} \frac{d\mu_2^G}{dt} &= k_{te} \left[(\mu_2^{RC} + \mu_2^{RCR}) (\mu_1^G - \mu_0^G) + (\mu_1^{RC} + \mu_1^{RCR}) (\mu_2^G - \mu_1^G) + \frac{1}{6} (\mu_0^{RC} + \mu_0^{RCR}) (-4\mu_3^G + 3\mu_2^G + \mu_1^G) \right] \\ &+ k_{de} \left[-\frac{1}{3} (4\mu_3^G - 3\mu_2^G - \mu_1^G) + \frac{1}{6} (2\mu_3^{RC} - 3\mu_2^{RC} + \mu_1^{RC}) + \frac{1}{6} (2\mu_3^{RCR} - 3\mu_2^{RCR} + \mu_1^{RCR}) \right. \\ &\quad \left. + \frac{1}{6} (2\mu_3^D - 3\mu_2^D + \mu_1^D) \right] \end{aligned} \quad (21)$$

For modeling the ROP, equations (1)-(5) and (10)-(21) need to be implemented together with the closure conditions (see paper).

Bi-functional co-initiator

For a simplified representation of the model equations, the following substitutions are introduced to account for the number of chain ends with catalyst and catalyst residue:

$$\mu_i^{\sum RC} = \mu_i^{RC} + \mu_i^{RC,CR} + 2\mu_i^{RC,C} \quad (22)$$

$$\mu_i^{\sum RCR} = \mu_i^{RCR} + \mu_i^{RC,CR} + 2\mu_i^{RCR,CR} \quad (23)$$

$$\mu_i^{\sum R} = \mu_i^{\sum RC} + \mu_i^{\sum RCR} \quad (24)$$

Mass balances for small molecules (isochoric, no in- and outgoing flows):

$$\frac{dM}{dt} = -k_{CM}CM - k_{C,p}M\mu_0^{\sum RC} - k_{CR,p}M\mu_0^{\sum RCR} + k_{C,d}\mu_0^{\sum RC} + k_{CR,d}\mu_0^{\sum RCR} \quad (25)$$

$$\frac{dC}{dt} = -k_{CM}CM - k_{C,a1}C (\mu_0^{RC} + \mu_0^{RCR} + 2\mu_0^D) + k_{C,a2}A\mu_0^{\sum RC} \quad (26)$$

$$\frac{dCR}{dt} = k_{CM}CM - k_{CR,a1}CR (\mu_0^{RC} + \mu_0^{RCR} + 2\mu_0^D) + k_{CR,a2}A\mu_0^{\sum RCR} \quad (27)$$

$$\frac{dAC}{dt} = -k_{C,a1}C (\mu_0^{RC} + \mu_0^{RCR} + 2\mu_0^D) + k_{C,a2}AC\mu_0^{\sum RC} \quad (28)$$

$$\frac{dACR}{dt} = -k_{CR,a1}CR (\mu_0^{RC} + \mu_0^{RCR} + 2\mu_0^D) + k_{CR,a2}ACR\mu_0^{\sum RCR} \quad (29)$$

The population balances are not shown due to lack of benefit. However, these lead to the following moment equations for moments 0 to 2:

Active chains with one catalyst chain end:

$$\frac{d\mu_0^{RC}}{dt} = 2k_{C,al}C\mu_0^D - k_{C,a2}A_C\mu_0^{RC} - k_{C,al}C\mu_0^{RC} - k_{CR,al}CR\mu_0^{RC} + k_{CR,a2}ACR\mu_0^{RC,CR} + 2k_{C,a2}A_C\mu_0^{RC,C} \quad (30)$$

$$\begin{aligned} \frac{d\mu_1^{RC}}{dt} &= 2k_{C,al}C\mu_1^D - k_{C,a2}A_C\mu_1^{RC} - k_{C,al}C\mu_1^{RC} - k_{CR,al}CR\mu_1^{RC} + k_{CR,a2}ACR\mu_1^{RC,CR} + 2k_{C,a2}A_C\mu_1^{RC,C} \\ &+ 2k_{C,p}M\mu_0^{RC} - 2k_{C,d}\mu_0^{RC} \\ &+ k_s \left[-\mu_1^{RC} \sum_{i \neq RC,G} \mu_0^i + \mu_0^{RC} \sum_{i \neq RC,G} \mu_1^i \right] \\ &+ k_{te} \left[-\mu_1^{RC} \sum_{i \neq RC} (\mu_1^i - \mu_0^i) + \frac{1}{2}\mu_0^{RC} \sum_{i \neq RC} (\mu_2^i - \mu_1^i) \right] \\ &- \frac{1}{2}k_{de} (\mu_2^{RC} - \mu_1^{RC}) \end{aligned} \quad (31)$$

$$\begin{aligned} \frac{d\mu_2^{RC}}{dt} &= 2k_{C,al}C\mu_2^D - k_{C,a2}A_C\mu_2^{RC} - k_{C,al}C\mu_2^{RC} - k_{CR,al}CR\mu_2^{RC} + k_{CR,a2}ACR\mu_2^{RC,CR} + 2k_{C,a2}A_C\mu_2^{RC,C} \\ &+ 4k_{C,p}M (\mu_1^{RC} + \mu_0^{RC}) + 4k_{C,d} (\mu_0^{RC} - \mu_1^{RC}) \\ &+ k_s \left[-\mu_2^{RC} \sum_{i \neq RC,G} \mu_0^i + \mu_0^{RC} \sum_{i \neq RC,G} \mu_2^i \right] \\ &+ k_{te} \left[\frac{1}{3}\mu_0^{RC} (\mu_1^{RC} - \mu_3^{RC}) + \mu_1^{RC} (\mu_2^{RC} - \mu_1^{RC}) - \mu_2^{RC} \sum_{i \neq RC} (\mu_1^i - \mu_0^i) + \frac{1}{6}\mu_0^{RC} \sum_{i \neq RC} (2\mu_3^i - 3\mu_2^i + \mu_1^i) \right] \\ &- \frac{1}{6}k_{de} (4\mu_3^{RC} - 3\mu_2^{RC} - \mu_1^{RC}) \end{aligned} \quad (32)$$

Active chains with one catalyst residue chain end:

$$\frac{d\mu_0^{RCR}}{dt} = 2k_{CR,al}C\mu_0^D - k_{CR,a2}ACR\mu_0^{RCR} - k_{CR,al}CR\mu_0^{RCR} - k_{C,al}C\mu_0^{RCR} + k_{C,a2}AC\mu_0^{RC,CR} + 2k_{CR,a2}ACR\mu_0^{RCR,CR} \quad (33)$$

$$\begin{aligned} \frac{d\mu_1^{RCR}}{dt} &= 2k_{CR,al}C\mu_1^D - k_{CR,a2}ACR\mu_1^{RCR} - k_{CR,al}CR\mu_1^{RCR} - k_{C,al}C\mu_1^{RCR} + k_{C,a2}AC\mu_1^{RC,CR} + 2k_{CR,a2}ACR\mu_1^{RCR,CR} \\ &+ 2k_{CR,p}M\mu_0^{RCR} - 2k_{CR,d}\mu_0^{RCR} \\ &+ k_s \left[-\mu_1^{RCR} \sum_{i \neq RCR,G} \mu_0^i + \mu_0^{RCR} \sum_{i \neq RCR,G} \mu_1^i \right] \\ &+ k_{te} \left[-\mu_1^{RCR} \sum_{i \neq RCR} (\mu_1^i - \mu_0^i) + \frac{1}{2}\mu_0^{RCR} \sum_{i \neq RCR} (\mu_2^i - \mu_1^i) \right] \\ &- \frac{1}{2}k_{de} (\mu_2^{RCR} - \mu_1^{RCR}) \end{aligned} \quad (34)$$

$$\begin{aligned} \frac{d\mu_2^{RCR}}{dt} &= 2k_{CR,al}C\mu_2^D - k_{CR,a2}ACR\mu_2^{RCR} - k_{CR,al}CR\mu_2^{RCR} - k_{C,al}C\mu_2^{RCR} + k_{C,a2}AC\mu_2^{RC,CR} + 2k_{CR,a2}ACR\mu_2^{RCR,CR} \\ &+ 4k_{CR,p}M (\mu_1^{RCR} + \mu_0^{RCR}) + 4k_{CR,d} (\mu_0^{RCR} - \mu_1^{RCR}) \\ &+ k_s \left[-\mu_2^{RCR} \sum_{i \neq RCR,G} \mu_0^i + \mu_0^{RCR} \sum_{i \neq RCR,G} \mu_2^i \right] \\ &+ k_{te} \left[\frac{1}{3}\mu_0^{RCR} (\mu_1^{RCR} - \mu_3^{RCR}) + \mu_1^{RCR} (\mu_2^{RCR} - \mu_1^{RCR}) - \mu_2^{RCR} \sum_{i \neq RCR} (\mu_1^i - \mu_0^i) + \frac{1}{6}\mu_0^{RCR} \sum_{i \neq RCR} (2\mu_3^i - 3\mu_2^i + \mu_1^i) \right] \\ &- \frac{1}{6}k_{de} (4\mu_3^{RCR} - 3\mu_2^{RCR} - \mu_1^{RCR}) \end{aligned} \quad (35)$$

Active chains with one catalyst and one catalyst residue chain end:

$$\frac{d\mu_0^{R_C,CR}}{dt} = k_{C,al}C\mu_0^{R_{CR}} - k_{C,a2}A_C\mu_0^{R_C,CR} + k_{CR,al}CR\mu_0^{R_C} - k_{CR,a2}A_{CR}\mu_0^{R_C,CR} \quad (36)$$

$$\begin{aligned} \frac{d\mu_1^{R_C,CR}}{dt} &= k_{C,al}C\mu_1^{R_{CR}} - k_{C,a2}A_C\mu_1^{R_C,CR} + k_{CR,al}CR\mu_1^{R_C} - k_{CR,a2}A_{CR}\mu_1^{R_C,CR} \\ &+ 2k_{C,p}M\mu_0^{R_C,CR} + 2k_{CR,p}M\mu_0^{R_C,CR} - 2k_{C,d}\mu_0^{R_C,CR} - 2k_{CR,d}\mu_0^{R_C,CR} \\ &+ k_s \left[-\mu_1^{R_C,CR} \sum_{i \neq R_C,CR,G} \mu_0^i + \mu_0^{R_C,CR} \sum_{i \neq R_C,CR,G} \mu_1^i \right] \\ &+ k_{te} \left[-\mu_1^{R_C,CR} \sum_{i \neq R_C,CR} (\mu_1^i - \mu_0^i) + \frac{1}{2}\mu_0^{R_C,CR} \sum_{i \neq R_C,CR} (\mu_2^i - \mu_1^i) \right] \\ &- \frac{1}{2}k_{de} (\mu_2^{R_C,CR} - \mu_1^{R_C,CR}) \end{aligned} \quad (37)$$

$$\begin{aligned} \frac{d\mu_2^{R_C,CR}}{dt} &= k_{C,al}C\mu_2^{R_{CR}} - k_{C,a2}A_C\mu_2^{R_C,CR} + k_{CR,al}CR\mu_2^{R_C} - k_{CR,a2}A_{CR}\mu_2^{R_C,CR} \\ &+ 4k_{C,p}M (\mu_1^{R_C,CR} + \mu_0^{R_C,CR}) + 4k_{CR,p}M (\mu_1^{R_C,CR} + \mu_0^{R_C,CR}) \\ &+ 4k_{C,d} (\mu_0^{R_C,CR} - \mu_1^{R_C,CR}) + 4k_{CR,d} (\mu_0^{R_C,CR} - \mu_1^{R_C,CR}) \\ &+ k_s \left[-\mu_2^{R_C,CR} \sum_{i \neq R_C,CR,G} \mu_0^i + \mu_0^{R_C,CR} \sum_{i \neq R_C,CR,G} \mu_2^i \right] \\ &+ k_{te} \left[\frac{1}{3}\mu_0^{R_C,CR} (\mu_1^{R_C,CR} - \mu_3^{R_C,CR}) + \mu_1^{R_C,CR} (\mu_2^{R_C,CR} - \mu_1^{R_C,CR}) \right. \\ &\quad \left. - \mu_2^{R_C,CR} \sum_{i \neq R_C,CR} (\mu_1^i - \mu_0^i) + \frac{1}{6}\mu_0^{R_C,CR} \sum_{i \neq R_C,CR} (2\mu_3^i - 3\mu_2^i + \mu_1^i) \right] \\ &- \frac{1}{6}k_{de} (4\mu_3^{R_C,CR} - 3\mu_2^{R_C,CR} - \mu_1^{R_C,CR}) \end{aligned} \quad (38)$$

Active chains with two catalyst chain ends:

$$\frac{d\mu_0^{R_{C,C}}}{dt} = k_{C,al}C\mu_0^{R_C} - 2k_{C,a2}A_C\mu_0^{R_{C,C}} \quad (39)$$

$$\begin{aligned} \frac{d\mu_1^{R_{C,C}}}{dt} = & k_{C,al}C\mu_1^{R_C} - 2k_{C,a2}A_C\mu_1^{R_{C,C}} + 2k_{C,p}M\mu_0^{R_{C,C}} - 2k_{C,d}\mu_0^{R_{C,C}} \\ & + k_s \left[-\mu_1^{R_{C,C}} \sum_{i \neq R_{C,C},G} \mu_0^i + \mu_0^{R_{C,C}} \sum_{i \neq R_{C,C},G} \mu_1^i \right] \\ & + k_{te} \left[-\mu_1^{R_{C,C}} \sum_{i \neq R_{C,C}} (\mu_1^i - \mu_0^i) + \frac{1}{2}\mu_0^{R_{C,C}} \sum_{i \neq R_{C,C}} (\mu_2^i - \mu_1^i) \right] \\ & - \frac{1}{2}k_{de} (\mu_2^{R_{C,C}} - \mu_1^{R_{C,C}}) \end{aligned} \quad (40)$$

$$\begin{aligned} \frac{d\mu_2^{R_{C,C}}}{dt} = & k_{C,al}C\mu_2^{R_C} - 2k_{C,a2}A_C\mu_2^{R_{C,C}} + 4k_{C,p}M (\mu_1^{R_{C,C}} + \mu_0^{R_{C,C}}) + 4k_{C,d} (\mu_0^{R_{C,C}} - \mu_1^{R_{C,C}}) \\ & + k_s \left[-\mu_2^{R_{C,C}} \sum_{i \neq R_{C,C},G} \mu_0^i + \mu_0^{R_{C,C}} \sum_{i \neq R_{C,C},G} \mu_2^i \right] \\ & + k_{te} \left[\frac{1}{3}\mu_0^{R_{C,C}} (\mu_1^{R_{C,C}} - \mu_3^{R_{C,C}}) + \mu_1^{R_{C,C}} (\mu_2^{R_{C,C}} - \mu_1^{R_{C,C}}) \right. \\ & \quad \left. - \mu_2^{R_{C,C}} \sum_{i \neq R_{C,C}} (\mu_1^i - \mu_0^i) + \frac{1}{6}\mu_0^{R_{C,C}} \sum_{i \neq R_{C,C}} (2\mu_3^i - 3\mu_2^i + \mu_1^i) \right] \\ & - \frac{1}{6}k_{de} (4\mu_3^{R_{C,C}} - 3\mu_2^{R_{C,C}} - \mu_1^{R_{C,C}}) \end{aligned} \quad (41)$$

Active chains with two catalyst residue chain ends:

$$\frac{d\mu_0^{R_{CR,CR}}}{dt} = k_{CR,a1}CR\mu_0^{R_{CR}} - 2k_{CR,a2}A_{CR}\mu_0^{R_{CR,CR}} \quad (42)$$

$$\begin{aligned} \frac{d\mu_1^{R_{CR,CR}}}{dt} = & k_{CR,a1}CR\mu_1^{R_{CR}} - 2k_{CR,a2}A_{CR}\mu_1^{R_{CR,CR}} + 2k_{CR,p}M\mu_0^{R_{CR,CR}} - 2k_{CR,d}\mu_0^{R_{CR,CR}} \\ & + k_s \left[-\mu_1^{R_{CR,CR}} \sum_{i \neq R_{CR,CR},G} \mu_0^i + \mu_0^{R_{CR,CR}} \sum_{i \neq R_{CR,CR},G} \mu_1^i \right] \\ & + k_{te} \left[-\mu_1^{R_{CR,CR}} \sum_{i \neq R_{CR,CR}} (\mu_1^i - \mu_0^i) + \frac{1}{2}\mu_0^{R_{CR,CR}} \sum_{i \neq R_{CR,CR}} (\mu_2^i - \mu_1^i) \right] \\ & - \frac{1}{2}k_{de} (\mu_2^{R_{CR,CR}} - \mu_1^{R_{CR,CR}}) \end{aligned} \quad (43)$$

$$\begin{aligned} \frac{d\mu_2^{R_{CR,CR}}}{dt} = & k_{CR,a1}CR\mu_2^{R_{CR}} - 2k_{CR,a2}A_{CR}\mu_2^{R_{CR,CR}} + 4k_{CR,p}M (\mu_1^{R_{CR,CR}} + \mu_0^{R_{CR,CR}}) + 4k_{CR,d} (\mu_0^{R_{CR,CR}} - \mu_1^{R_{CR,CR}}) \\ & + k_s \left[-\mu_2^{R_{CR,CR}} \sum_{i \neq R_{CR,CR},G} \mu_0^i + \mu_0^{R_{CR,CR}} \sum_{i \neq R_{CR,CR},G} \mu_2^i \right] \\ & + k_{te} \left[\frac{1}{3}\mu_0^{R_{CR,CR}} (\mu_1^{R_{CR,CR}} - \mu_3^{R_{CR,CR}}) + \mu_1^{R_{CR,CR}} (\mu_2^{R_{CR,CR}} - \mu_1^{R_{CR,CR}}) \right. \\ & \quad \left. - \mu_2^{R_{CR,CR}} \sum_{i \neq R_{CR,CR}} (\mu_1^i - \mu_0^i) + \frac{1}{6}\mu_0^{R_{CR,CR}} \sum_{i \neq R_{CR,CR}} (2\mu_3^i - 3\mu_2^i + \mu_1^i) \right] \\ & - \frac{1}{6}k_{de} (4\mu_3^{R_{CR,CR}} - 3\mu_2^{R_{CR,CR}} - \mu_1^{R_{CR,CR}}) \end{aligned} \quad (44)$$

Inactive chains:

$$\frac{d\mu_0^D}{dt} = -k_{C,a1}C\mu_0^D + k_{C,a2}A_{C}\mu_0^{R_C} - k_{CR,a1}CR\mu_0^D + k_{CR,a2}A_{CR}\mu_0^{R_{CR}} + k_{CM}CM \quad (45)$$

$$\begin{aligned} \frac{d\mu_1^D}{dt} = & -k_{C,a1}C\mu_1^D + k_{C,a2}A_{C}\mu_1^{R_C} - k_{CR,a1}CR\mu_1^D + k_{CR,a2}A_{CR}\mu_1^{R_{CR}} + 2k_{CM}CM \\ & + k_s \left[\sum_{i \neq D,G} \mu_1^i \mu_0^D - \sum_{i \neq D,G} \mu_0^i \mu_1^D \right] \\ & + k_{te} \left[- \sum_{i \neq D,G} \mu_1^i (\mu_1^D - \mu_0^D) - \frac{1}{2} \sum_{i \neq D,G} \mu_1^i (\mu_2^D - \mu_1^D) \right] \\ & - \frac{1}{2}k_{de} (\mu_2^D - \mu_1^D) \end{aligned} \quad (46)$$

$$\begin{aligned} \frac{d\mu_2^D}{dt} = & -k_{C,a1}C\mu_2^D + k_{C,a2}A_{C}\mu_2^{R_C} - k_{CR,a1}CR\mu_2^D + k_{CR,a2}A_{CR}\mu_2^{R_{CR}} + 4k_{CM}CM \\ & + k_s \left[\sum_{i \neq D,G} \mu_2^i \mu_0^D - \sum_{i \neq D,G} \mu_0^i \mu_2^D \right] \\ & + k_{te} \left[\sum_{i \neq D,G} \mu_1^i (\mu_2^D - \mu_1^D) + \sum_{i \neq D,G} \mu_2^i (\mu_1^D - \mu_0^D) + \frac{1}{6} \sum_{i \neq D,G} \mu_0^i (-4\mu_3^D + 3\mu_2^D + \mu_1^D) \right] \\ & - \frac{1}{6}k_{de} (4\mu_3^D - 3\mu_2^D - \mu_1^D) \end{aligned} \quad (47)$$

Terminated chains:

$$\frac{d\mu_0^G}{dt} = k_{de} \sum_{i \neq G} (\mu_1^i - \mu_0^i) \quad (48)$$

$$\frac{d\mu_1^G}{dt} = k_{te} \left[\sum_{i \neq D, G} \mu_1^i (\mu_1^G - \mu_0^G) - \frac{1}{2} \sum_{i \neq D, G} \mu_0^i (\mu_2^G - \mu_1^G) \right] + k_{de} \left[(\mu_1^G - \mu_2^G) + \frac{1}{2} \sum_{i \neq G} (\mu_2^i - \mu_1^i) \right] \quad (49)$$

$$\begin{aligned} \frac{d\mu_2^G}{dt} = & k_{te} \left[\sum_{i \neq D, G} \mu_2^i (\mu_1^G - \mu_0^G) + \sum_{i \neq D, G} \mu_1^i (\mu_2^G - \mu_1^G) + \frac{1}{6} \sum_{i \neq D, G} \mu_0^i (-4\mu_3^G + 3\mu_2^G + \mu_1^G) \right] \\ & + k_{de} \left[-\frac{1}{3} (4\mu_3^G - 3\mu_2^G - \mu_1^G) + \frac{1}{6} \sum_{i \neq G} (2\mu_3^i - 3\mu_2^i + \mu_1^i) \right] \quad (50) \end{aligned}$$

For modeling, the equations (22)-(50) need to be implemented together with the closure conditions (see paper).

Reference

[S1] N. Conen, M. Fuchs, A. Hoffmann, S. Herres-Pawlis, Andreas Jupke, *Adv. Sustainable Syst.* **2023**, *7*, 2200359.

[S2] T. Biela, A. Duda, S. Penczek, Control of Mn, Mw/Mn, end-groups, and kinetics in living polymerization of cyclic esters, *Macromol. Symp.* **2002**, *183*, 1 – 10.

[S3] Peaxact, **2019**.